PHYSICAL REVIEW B **95**, 161114(R) (2017)

Measuring topological invariants from generalized edge states in polaritonic quasicrystals

Florent Baboux,[1,*] Eli Levy,[2,3] Aristide Lemaître,[1] Carmen Gómez,[1] Elisabeth Galopin,[1] Luc Le Gratiet,[1] Isabelle Sagnes,[1] Alberto Amo,[1] Jacqueline Bloch,[1] and Eric Akkermans[2]

[1]*Centre de Nanosciences et de Nanotechnologies, CNRS, Université Paris-Sud, Université Paris-Saclay, C2N Marcoussis, F-91460 Marcoussis, France*

[2]*Department of Physics, Technion Israel Institute of Technology, Haifa 32000, Israel*

[3]*Rafael Limited, P.O. Box 2250, Haifa 32100, Israel*

(Received 13 July 2016; revised manuscript received 3 March 2017; published 26 April 2017)

We investigate the topological properties of Fibonacci quasicrystals using cavity polaritons. Composite structures made of the concatenation of two Fibonacci sequences allow one to investigate generalized edge states forming in the gaps of the fractal energy spectrum. We employ these generalized edge states to determine the topological invariants of the quasicrystal. When varying a structural degree of freedom (phason) of the Fibonacci sequence, the edge states spectrally traverse the gaps, while their spatial symmetry switches: The periodicity of this spectral and spatial evolution yields direct measurements of the gap topological numbers. The topological invariants that we determine coincide with those assigned by the gap-labeling theorem, illustrating the direct connection between the fractal and topological properties of Fibonacci quasicrystals.

DOI: 10.1103/PhysRevB.95.161114

Topology has long been recognized as a powerful tool both in mathematics and in physics. It allows one to identify families of structures which cannot be related by continuous deformations and are characterized by integer numbers called topological invariants. A physical example where topological features are particularly useful is provided by quantum anomalies, i.e., classical symmetries broken at the quantum level [1], such as the chiral anomaly recently observed in condensed matter [2]. From a general viewpoint, wave or quantum systems possessing a gapped energy spectrum, such as band insulators, superconductors, or two-dimensional (2D) conductors in a magnetic field, can be assigned topological invariants, generally called Chern numbers [3]. These numbers control a variety of physical phenomena: For instance, in the integer quantum Hall effect, they determine the value of the Hall conductance as a function of magnetic field [4,5]. Such topological features related to Chern numbers have been explored in crystals [6] and more recently in various artificial periodic lattices for cold atoms [7–9], acoustic waves [10], or photons [11–16].

Quasicrystals—nonperiodic structures with long range order [17,18]—are another important class of systems exhibiting topological effects [19–24]. In particular, the topological edge states [25–27] of quasicrystals have been recently investigated in photonic systems [22,28–30] and exploited to implement topological pumping, a key concept of topology [22]. A paradigmatic example of a quasicrystal is given by the one-dimensional (1D) Fibonacci chain. It presents a fractal energy spectrum which consists of an infinite number of gaps [31]. A rather surprising and fascinating property is that each of these gaps can also be assigned a topological number analogous to the aforementioned Chern numbers [32]: This constitutes the so-called gap-labeling theorem [33]. These integers can take N distinct values, N being the number of letters in the chain [34]. Despite important advances on the topological properties of quasicrystals [19–24,28–30], the topological invariants have not yet been directly measured as winding numbers.

The physical origin of topological numbers in a Fibonacci quasicrystal can be related to its structural properties [35]. To understand this, let us introduce a general method to generate a Fibonacci sequence: It is based on the characteristic function

$$\chi_j = \mathrm{sgn}[\cos(2\pi j\sigma^{-1} + \phi) - \cos(\pi\sigma^{-1})], \qquad (1)$$

proposed in Ref. [36], which takes two possible values ± 1, respectively identified with two letters A and B representing, e.g., two different values of a potential energy. A Fibonacci sequence of size N is a word $\overrightarrow{F_N}(\phi) \equiv [\chi_1\chi_2\cdots\chi_N]$ formed by A and B letters. In Eq. (1), $\sigma = (1+\sqrt{5})/2$ is the golden mean and ϕ is a structural degree of freedom called a phason, which can be continuously varied between 0 and 2π. The role of the phason has been experimentally investigated in the frame of the Harper tight-binding model [22,28,36]. In the case of the Fibonacci model, ϕ allows one to select distinct finite segments along the infinite chain $\overrightarrow{F}_\infty$. Sweeping ϕ over a 2π period induces a series of N independent local structural changes in the Fibonacci sequence $\overrightarrow{F_N}$. Each change corresponds to the exchange of two letters ($AB \leftrightarrow BA$) at a given location of the sequence [see the vertical arrows in Fig. 1(c)]. Importantly, for two particular values of ϕ within a period, the Fibonacci sequence $\overrightarrow{F_N}(\phi)$ becomes palindromic, i.e., it coincides with its mirror symmetric $\overleftarrow{F_N}(\phi) = [\chi_N\chi_{N-1}\cdots\chi_1]$. In between these two values, ϕ drives a π-periodic symmetry cycle along the 1D structure. When concatenating $\overrightarrow{F_N}(\phi)$ with $\overleftarrow{F_N}(\phi)$, generalized edge states appear at the interface of the two mirror sequences, with properties tightly linked to ϕ. Since topological invariants can always be written as winding numbers, it was predicted [35] that the Fibonacci topological numbers are measurable by counting how many times the edge states traverse the gap while scanning the phason degree of freedom.

In this Rapid Communication we present a direct measurement of the topological invariants of a Fibonacci quasicrystal as spectral winding numbers. As an important consequence,

*Present address: Laboratoire Matériaux et Phénomènes Quantiques, Université Paris Diderot.

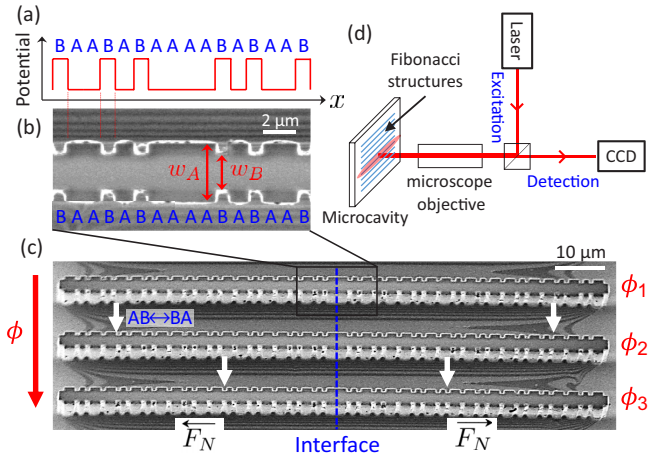

FIG. 1. (a) Nominal potential energy corresponding to a laterally modulated 1D cavity. (b) SEM image of a portion of a 1D cavity reproducing the Fibonacci sequence (top view). The letters A and B correspond to two different widths of the cavity. (c) SEM image showing the full view of three fabricated Fibonacci structures, corresponding to three different values of the phason ϕ. Each structure consists of the concatenation $\overleftarrow{F_N}\overrightarrow{F_N}$ of a Fibonacci sequence $\overrightarrow{F_N}$ and its mirror symmetric $\overleftarrow{F_N}$. Vertical white arrows indicate the position of local changes in the sequence introduced when scanning ϕ. (d) Schematics of the experimental setup.

we also relate these invariants to the observed change of spatial symmetry of generalized edge states, a robust feature largely insensitive to intrinsic disorder and other imperfections. We employ cavity polaritons, quasiparticles arising from the strong coupling between excitons confined in quantum wells and photons confined in a semiconductor microcavity [37]. This photonic system allows one to emulate a variety of Hamiltonians [38–41] and characterize the associated eigenstates both in the spectral and spatial domain [40]. Here, we harness these features to emulate generalized edge states forming in the gaps of the fractal Fibonacci spectrum.

To explore the edge states, we design concatenated structures $\overleftarrow{F_N}\overrightarrow{F_N}$ made of the juxtaposition of a given Fibonacci sequence and its mirror symmetric [Fig. 1(c)]. The interface defines a Fabry-Pérot cavity of zero geometric length but finite round-trip phase $\theta_{\rm cav}$ due to the reflexion between $\overrightarrow{F_N}$ and $\overleftarrow{F_N}$ (see Supplemental Material [42]). Thus, the edge states will appear at energies $E_{\rm gap}(\phi)$, implicitly determined by the resonance condition

$$\theta_{\rm cav}(E_{\rm gap},\phi) = 2\pi m, \tag{2}$$

with $m \in \mathbb{Z}$. As detailed in Ref. [35], $\theta_{\rm cav}$ is periodic in ϕ with a period $\frac{\pi}{|q|}$, where q is an integer, the topological invariant of the considered gap. Therefore, the evolution of the energy of the edge states when increasing ϕ reflects directly the topological properties of the gap in which they appear.

To fabricate these structures, we process a planar microcavity (of nominal Q factor 70 000) grown by molecular beam epitaxy. The cavity consists of a $\lambda/2$ $Ga_{0.05}Al_{0.95}As$ layer surrounded by two $Ga_{0.8}Al_{0.2}As/Ga_{0.05}Al_{0.95}As$ Bragg mirrors with 28 and 40 pairs in the top and bottom mirrors, respectively. Twelve GaAs quantum wells of 7 nm width are inserted in the structure, resulting in a 15 meV Rabi splitting. Quasi-1D cavities (wires) are realized using electron beam lithography and dry etching. The lateral width of these wires is modulated quasiperiodically, as shown in the scanning electron microscopy (SEM) image of Fig. 1(b). The modulation consists of two wire sections A and B of same length $a = 1$ μm, but different widths w_A and w_B. The width modulation induces an effective 1D potential for the longitudinal motion of polaritons [Fig. 1(a)] that follows the desired Fibonacci sequence. We chose $N = 55$ letters for the Fibonacci sequences and thus 110 letters for the concatenated structures. We have fabricated on a single sample the $N = 55$ concatenated structures corresponding to all possible values of ϕ producing a structural change in the sequence. Figure 1(c) shows a subset of three fabricated structures; the position of the interface between the mirror sequences $\overleftarrow{F_N}$ and $\overrightarrow{F_N}$ is indicated by a vertical line. The exciton-photon detuning is of the order of -20 meV for all experiments.

To study the polariton modes in these quasiperiodic structures, we perform low temperature (10 K) microphotoluminescence experiments [see Fig. 1(d)]. Single structures are excited nonresonantly at low power, using a cw monomode laser at 740 nm. The excitation spot covers an 80-μm-long region centered on the interface. The emission is collected with a 0.5 numerical aperture objective and focused on the entrance slit of a spectrometer coupled to a CCD camera. Imaging the sample surface or the Fourier plane of the collection objective allows one to study the polariton modes either in real or momentum space.

Figure 2 shows the photoluminescence spectrum in real space [Fig. 2(a)] and momentum space [Fig. 2(b)] of a Fibonacci structure with $\phi = 0.6\pi$, $w_A = 3.5$ μm, and $w_B = 2.2$ μm. The energy spectrum shows an alternation of minibands and gaps. The emission in real space allows one to identify two types of modes in the spectrum: modes delocalized over the whole structure, and modes localized at the interface between the $\overleftarrow{F_N}$ and $\overrightarrow{F_N}$ sequences ($x = 0$). The delocalized modes form minibands, as can be seen in the momentum space emission: These modes are bulk modes forming a fractal energy spectrum characteristic of the Fibonacci quasicrystal [43]. We can identify the main gaps of the spectrum by applying the gap-labeling theorem [33], which predicts $k = \frac{\pi}{a}(p + q\sigma^{-1})$ for the wave-vector position of the gaps [44]. Here, p and q are integers, with q being the gap topological number [33]. From the momentum space spectrum of Fig. 2(b) we extract $[p,q] = [-1,2]$ for the lower main energy gap, and $[p,q] = [1,-1]$ for the higher main energy gap.

In addition to the bulk states, we observe states that are localized at the interface between $\overleftarrow{F_N}$ and $\overrightarrow{F_N}$. One of them (at energy $\sim$1596.5 meV) lies below the bulk band structure and is thus topologically trivial [42]. Two other localized states (encircled) lie within the widest spectral gaps: These are the expected topological edge states. Their spatial localization around the interface depends on the contrast of the Fibonacci quasiperiodic potential. Figure 2(c) shows the spatial profile [squared modulus of the wave function $|\psi(x)|^2$] of the edge state of the gap $q = +2$, measured for a series of structures of the same A-letter width $w_A = 3.5$ μm, but various B-letter widths w_B. As w_B decreases, the potential contrast [amplitude

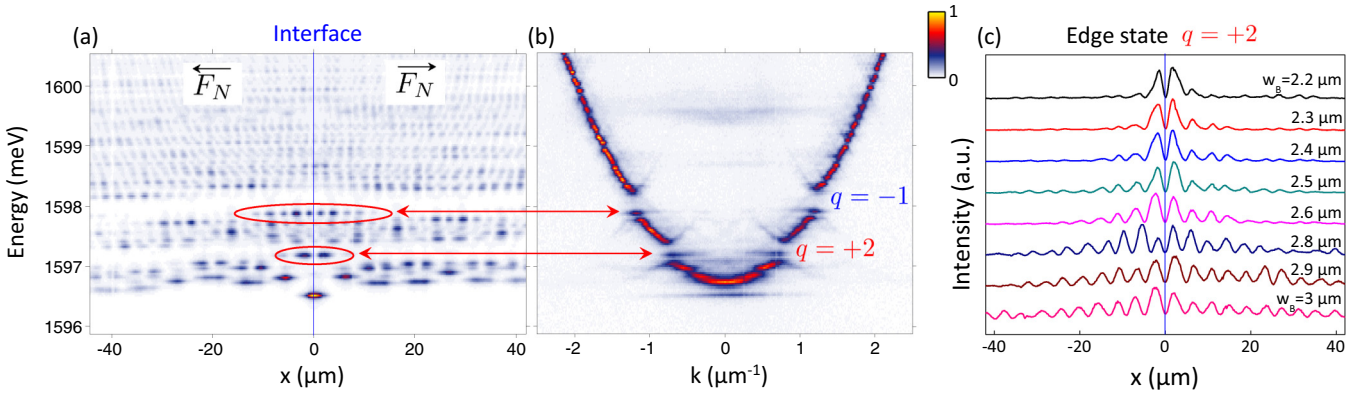

FIG. 2. (a), (b) Energy-resolved emission of a Fibonacci structure (a) in real space and (b) in momentum space, for a given value of the phason ($\phi = 0.62\pi$). Edge states are visible in the two lowest main energy gaps, characterized by $q = +2$ and $q = -1$. These states are localized at the interface ($x = 0$) between the $\overleftarrow{F_N}$ and $\overrightarrow{F_N}$ Fibonacci sequences. (c) Spatial profile of the edge state of gap $q = +2$ measured in a series of structures of the same A-letter width $w_A = 3.5$ μm but various B-letter widths w_B, yielding different contrasts for the Fibonacci potential.

of the steps in Fig. 1(a)] increases: This leads to wider spectral gaps, and thus to a stronger spatial localization of the wave function.

To explore the topological properties of the Fibonacci sequences by means of these edge states, we will now monitor their evolution when varying the phason degree of freedom ϕ. We investigate a full set of $N = 55$ structures with $w_A = 3.5$ μm and $w_B = 2.4$ μm. For each structure, we perform spectroscopic measurements similar to Figs. 2(a) and 2(b), and extract the energy of the two edge states with respect to the lowest bulk energy mode (bottom of the parabola, energy E_0). The results are plotted in Fig. 3(a), where the gap boundaries are indicated by the horizontal lines. Numerical calculations based on a scattering matrix approach [35] are presented for comparison in Fig. 3(c). Note that when $\phi = 0$ or π, no edge state is observed. Indeed, for these particular values of ϕ, the $\overrightarrow{F_N}$ sequence is palindromic and $\overleftarrow{F_N}\,\overrightarrow{F_N}$ effectively reduces to a single Fibonacci sequence of size $2N$. Hence there is no interface cavity and thus no edge state.

As clearly seen in Fig. 3(a), while scanning the phason ϕ, the states perform piecewise spectral traverses inside the gaps. The number and the direction of the traverses yield a direct determination of the winding number [35],

$$\mathcal{W} = \frac{1}{2\pi}\int_0^{2\pi} \frac{d\theta_{\rm cav}}{d\phi} d\phi = \frac{1}{2\pi}\int_0^{2\pi} \frac{d\tilde{\delta}}{d\phi} d\phi = 2q, \qquad (3)$$

where $\tilde{\delta} \equiv \frac{E_{\rm gap} - E_-}{\Delta_g}$ is the relative spectral position of the edge state within the gap, with Δ_g being the gap width and E_- the energy of the gap lower boundary [45].

The direction and periodicity of the observed traverse are different for the two edge states we consider: The lower energy state traverses upwards four times (winding number $\mathcal{W} = +4$), while the higher energy state traverses downwards two times ($\mathcal{W} = -2$), when ϕ spans a full period $[0, 2\pi]$. This winding $\mathcal{W} = 2q$ of the edge states allows for a direct determination of the gap topological numbers. We deduce $q = +2$ for the lower energy state and $q = -1$ for the higher energy state. These values obtained from the winding of the *edge* states are fully consistent with those previously determined from the *bulk* band structure (gap-labeling theorem), illustrating the existence of a bulk-edge correspondence in the quasiperiodic system.

We now show that the topological invariants of the quasicrystal are not only measurable as winding numbers of the edge states, but they can also be directly retrieved from the spatial symmetry of the corresponding wave functions. Figure 4 (left column) shows the measured profile of the $q = +2$ and $q = -1$ edge states for values of ϕ taken in

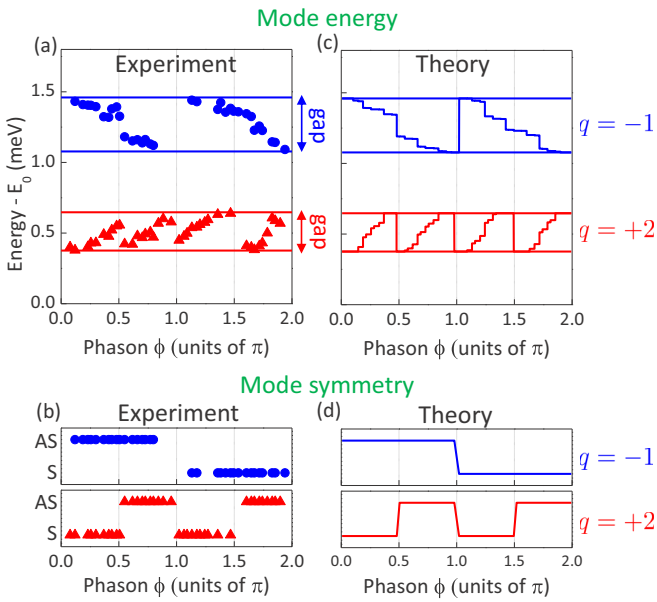

FIG. 3. (a) Measured energy of the edge states of gaps $q = +2$ and $q = -1$ as a function of the phason ϕ. E_0 denotes the energy of the lowest bulk mode, and the solid lines indicate the gap boundaries. (b) Corresponding spatial symmetry of the edge states. When scanning ϕ, the wave functions evolve from symmetric (S) to antisymmetric (AS) with respect to the interface ($x = 0$). (c) Relative spectral position within the gaps of the two considered edge states, obtained from scattering matrix calculations. (d) Calculated symmetry of the two considered edge states.

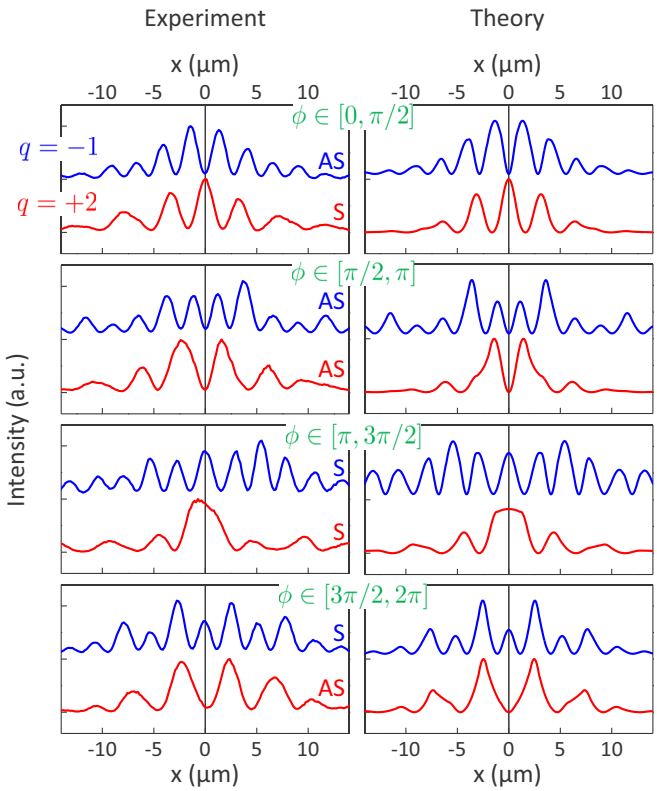

FIG. 4. Measured (left) and calculated (right) spatial profile of the $q = +2$ and $q = -1$ edge states for values of ϕ taken in four different quadrants: $[0,\pi/2]$, $[\pi/2,\pi]$, $[\pi,3\pi/2]$, and $[3\pi/2,2\pi]$. The mode spatial structure switches from symmetric (S) to antisymmetric (AS) with respect to the interface ($x = 0$), with a direction and periodicity yielding a direct measurement of the topological invariants of the quasicrystal. The blue lines are shifted vertically to improve their visibility.

four successive quadrants: $[0,\pi/2]$, $[\pi/2,\pi]$, $[\pi,3\pi/2]$, and $[3\pi/2,2\pi]$. The states either show a maximum or a minimum intensity at the interface ($x = 0$), corresponding to either a node or an antinode of the wave function. In the frame of a Fabry-Pérot model [46] we will denote these two cases as symmetric (S) and antisymmetric (AS), respectively. Because of experimental imperfections the states are not perfectly S or AS, but we shall employ this convenient terminology. We observe that the $q = +2$ state (red) switches symmetry in each quadrant, while the $q = -1$ state (blue) keeps the same symmetry in the first two quadrants before switching to the opposite symmetry in the last two quadrants. The symmetry index (S or AS) is reported in Fig. 3(b) for all values of ϕ, and compared to theory in Fig. 3(d). Comparing this behavior to the spectral features reported in Figs. 3(a)–3(c), we observe that symmetry flips are exactly synchronized with the spectral traverse of the states: They occur in between two successive traverses. Their periodicity thus allows one to determine the absolute value of the topological numbers. In addition, we observe that the sign of q is reflected in the direction of the symmetry flips within a period: The wave function of the $q = -1$ state switches from AS to S while that of the $q = +2$ state switches from S to AS. These experimental observations can be fully accounted for by a Fabry-Pérot interpretation. The resonance condition of Eq. (2), besides giving an accurate prediction for the gap state energies as shown in Figs. 3(a) and 3(c), also encodes information on the mode symmetry. Indeed, for a fixed cavity length the occurrence of a node or antinode at the center is fully determined by the parity of the integer m. The spatial symmetry of the topological states thus switches at each spectral traverse [42]. This can be seen in the right column of Fig. 4, showing the calculated spatial profile of the two gap states under study, in all four quadrants. These features demonstrate that, in contrast to previous studies using normal edges (interface with vacuum) [22,29], the use of generalized edges yields an additional degree of freedom (the symmetry index) that can be used to directly measure the topological invariants of the quasicrystal. This method is independent from the one based on spectral windings. It should thus prove useful in other physical platforms where the spectral degrees of freedom are more difficult to access.

In summary, we have investigated the topological properties of 1D Fibonacci polaritonic quasicrystals. We image generalized edge states forming in the gaps of the fractal energy spectrum. The behavior of these edge states upon varying a structural degree of freedom (phason) allows for a direct determination of the topological invariants of the quasicrystal. The latter coincide with the bulk invariants assigned by the gap-labeling theorem, illustrating the direct connection between the fractal and topological properties of Fibonacci quasicrystals. This work establishes a method to determine the topological features of quasicrystals by means of a direct measurement of winding numbers and of the corresponding symmetry flips of the wave functions. Taking advantage of the matter part of polaritons, it could be extended to probe the interplay of topology and interactions in quasicrystals [47] and potentially realize strongly correlated topological phases [48]. Furthermore, the building of cavities with topological mirrors could allow for the investigation of the topological Casimir effect [49] in a well-controlled platform.

This work was supported by the Israel Science Foundation Grant No. 924/09, by the Agence Nationale de la Recherche projects *Quandyde* (Grant No. ANR-11-BS10-001) and *Quantum Fluids of Light* (Grant No. ANR-16-CE30-0021), the French *RENATECH* network, the European Research Council grant *Honeypol*, and the EU-FET Proactive grant *AQuS* (Project No. 640800).

F.B. and E.L. contributed equally to this work.

[1] D. J. Gross and R. Jackiw, Phys. Rev. D **6**, 477 (1972).

[2] J. Xiong, S. K. Kushwaha, T. Liang, J. W. Krizan, M. Hirschberger, W. Wang, R. Cava, and N. Ong, Science **350**, 413 (2015).

[3] S. S. Chern, *Complex Manifolds Without Potential Theory* (Springer, New York, 1979).

[4] K. v. Klitzing, G. Dorda, and M. Pepper, Phys. Rev. Lett. **45**, 494 (1980).

[5] J. Bellissard, A. van Elst, and H. Schulz-Baldes, J. Math. Phys. **35**, 5373 (1994).
[6] M. Z. Hasan and C. L. Kane, Rev. Mod. Phys. **82**, 3045 (2010).
[7] N. Goldman, J. Dalibard, A. Dauphin, F. Gerbier, M. Lewenstein, P. Zoller, and I. B. Spielman, Proc. Natl. Acad. Sci. USA **110**, 6736 (2013).
[8] M. Atala, M. Aidelsburger, J. T. Barreiro, D. Abanin, T. Kitagawa, E. Demler, and I. Bloch, Nat. Phys. **9**, 795 (2013).
[9] M. Aidelsburger, M. Lohse, C. Schweizer, M. Atala, J. T. Barreiro, S. Nascimbene, N. Cooper, I. Bloch, and N. Goldman, Nat. Phys. **11**, 162 (2015).
[10] M. Xiao, G. Ma, Z. Yang, P. Sheng, Z. Zhang, and C. T. Chan, Nat. Phys. **11**, 240 (2015).
[11] M. C. Rechtsman, J. M. Zeuner, Y. Plotnik, Y. Lumer, D. Podolsky, F. Dreisow, S. Nolte, M. Segev, and A. Szameit, Nature (London) **496**, 196 (2013).
[12] M. Hafezi, Phys. Rev. Lett. **112**, 210405 (2014).
[13] W. Hu, J. C. Pillay, K. Wu, M. Pasek, P. P. Shum, and Y. D. Chong, Phys. Rev. X **5**, 011012 (2015).
[14] C. Poli, M. Bellec, U. Kuhl, F. Mortessagne, and H. Schomerus, Nat. Commun. **6**, 6710 (2015).
[15] S. A. Skirlo, L. Lu, Y. Igarashi, Q. Yan, J. Joannopoulos, and M. Soljačić, Phys. Rev. Lett. **115**, 253901 (2015).
[16] S. Mittal, S. Ganeshan, J. Fan, A. Vaezi, and M. Hafezi, Nat. Photonics **10**, 180 (2016).
[17] D. Shechtman, I. Blech, D. Gratias, and J. W. Cahn, Phys. Rev. Lett. **53**, 1951 (1984).
[18] D. Levine and P. J. Steinhardt, Phys. Rev. Lett. **53**, 2477 (1984).
[19] B. Simon, Adv. Appl. Math. **3**, 463 (1982).
[20] H. Kunz, Phys. Rev. Lett. **57**, 1095 (1986).
[21] L.-J. Lang, X. Cai, and S. Chen, Phys. Rev. Lett. **108**, 220401 (2012).
[22] Y. E. Kraus, Y. Lahini, Z. Ringel, M. Verbin, and O. Zilberberg, Phys. Rev. Lett. **109**, 106402 (2012).
[23] Y. E. Kraus, Z. Ringel, and O. Zilberberg, Phys. Rev. Lett. **111**, 226401 (2013).
[24] S. Ganeshan, K. Sun, and S. Das Sarma, Phys. Rev. Lett. **110**, 180403 (2013).
[25] E. S. Zijlstra, A. Fasolino, and T. Janssen, Phys. Rev. B **59**, 302 (1999).
[26] Y. El Hassouani, H. Aynaou, E. H. El Boudouti, B. Djafari-Rouhani, A. Akjouj, and V. R. Velasco, Phys. Rev. B **74**, 035314 (2006).
[27] X.-N. Pang, J.-W. Dong, and H.-Z. Wang, J. Opt. Soc. Am. B **27**, 2009 (2010).
[28] M. Verbin, O. Zilberberg, Y. E. Kraus, Y. Lahini, and Y. Silberberg, Phys. Rev. Lett. **110**, 076403 (2013).
[29] M. Verbin, O. Zilberberg, Y. Lahini, Y. E. Kraus, and Y. Silberberg, Phys. Rev. B **91**, 064201 (2015).
[30] P. Vignolo, M. Bellec, J. Böhm, A. Camara, J.-M. Gambaudo, U. Kuhl, and F. Mortessagne, Phys. Rev. B **93**, 075141 (2016).
[31] D. Damanik, M. Embree, A. Gorodetski, and S. Tcheremchantsev, Commun. Math. Phys. **280**, 499 (2008).
[32] Note that, strictly speaking, Chern numbers are invariants describing the topology of smooth Riemannian manifolds. In contrast, the Fibonacci chain and quasicrystals in general cannot be ascribed such a smooth manifold but rather discrete graphs [50] whose topological numbers are termed differently (K-theory invariants). For simplicity, we shall pursue using indifferently the denomination Chern numbers or topological numbers.
[33] J. Bellissard, A. Bovier, and J.-M. Ghez, Rev. Math. Phys. **4**, 1 (1992).
[34] A. Dareau, E. Levy, M. Bosch Aguilera, R. Bouganne, E. Akkermans, F. Gerbier, and J. Beugnon, arXiv:1607.00901.
[35] E. Levy, A. Barak, A. Fisher, and E. Akkermans, arXiv:1509.04028.
[36] Y. E. Kraus and O. Zilberberg, Phys. Rev. Lett. **109**, 116404 (2012).
[37] C. Weisbuch, M. Nishioka, A. Ishikawa, and Y. Arakawa, Phys. Rev. Lett. **69**, 3314 (1992).
[38] M. Bayer, T. Gutbrod, A. Forchel, T. L. Reinecke, P. A. Knipp, R. Werner, and J. P. Reithmaier, Phys. Rev. Lett. **83**, 5374 (1999).
[39] N. Y. Kim, K. Kusudo, C. Wu, N. Masumoto, A. Löffler, S. Höfling, N. Kumada, L. Worschech, A. Forchel, and Y. Yamamoto, Nat. Phys. **7**, 681 (2011).
[40] I. Carusotto and C. Ciuti, Rev. Mod. Phys. **85**, 299 (2013).
[41] F. Baboux, L. Ge, T. Jacqmin, M. Biondi, E. Galopin, A. Lemaître, L. Le Gratiet, I. Sagnes, S. Schmidt, H. E. Türeci, A. Amo, and J. Bloch, Phys. Rev. Lett. **116**, 066402 (2016).
[42] See Supplemental Material at http://link.aps.org/supplemental/10.1103/PhysRevB.95.161114 for details on the Fabry-Pérot interpretation and additional data.
[43] D. Tanese, E. Gurevich, F. Baboux, T. Jacqmin, A. Lemaître, E. Galopin, I. Sagnes, A. Amo, J. Bloch, and E. Akkermans, Phys. Rev. Lett. **112**, 146404 (2014).
[44] This property, exact in the limit of infinite chains, constitutes an excellent approximation for the considered structure length, as shown in Ref. [43].
[45] Since the quasicrystal is an effectively discrete manifold, the phase θ_{cav} defined in Eq. (2) can take only a finite set of discrete values equal to the Fibonacci number F_N. Thus, strictly speaking, the winding number $\mathcal{W}$ should be written as a discrete sum. As a convenient notation which results from the use of a continuous variable ϕ in Eq. (1), we replace this discrete sum by an integral.
[46] E. Levy and E. Akkermans, arXiv:1610.09562.
[47] B. Freedman, G. Bartal, M. Segev, R. Lifshitz, D. N. Christodoulides, and J. W. Fleischer, Nature (London) **440**, 1166 (2006).
[48] X.-G. Wen, Adv. Phys. **44**, 405 (1995).
[49] M. Bordag, G. L. Klimchitskaya, U. Mohideen, and V. M. Mostepanenko, *Advances in the Casimir Effect* (Oxford University Press, Oxford, UK, 2009).
[50] J. E. Anderson and I. F. Putnam, Ergodic Theory Dyn. Syst. **18**, 509 (1998).